

**APPENDIX G**

**ANALYSIS OF MAYSVILLE AND I-40 BRIDGES  
FOR WIND LOADS**

**By Mark Hunter**



**FINAL REPORT**  
**DETERMINATION OF HORIZONTAL**  
**WIND LOADS ON BRIDGES**  
**NCHRP 48**

**Project Number:** 99-267  
**Date:** October 13, 2000  
**Submitted By:** Rowan Williams Davies & Irwin Inc.  
Project Manager -Mark A. Hunter, CET  
Project Director - Peter A. Irwin, Ph.D., P.Eng.

---

**Submitted to:** Imbsen & Associates/Buckland & Taylor

---

**Rowan Williams  
Davies & Irwin Inc.**

Consulting Engineers  
650 Woodlawn Road West  
Guelph, Ontario  
Canada N1K 1B8  
Tel: (519) 823-1311  
Fax: (519) 823-1316  
Email: [info@rwdi.com](mailto:info@rwdi.com)  
Website: <http://www.rwdi.com>

## TABLE OF CONTENTS

1. Introduction
2. Determination of Transverse Wind Loads on Bridges
  - 2.1 Determination of Buffeting Response Using Quasi-Static Theory
  - 2.2 Determination of Buffeting Response Using Full Aeroelastic Model Tests
3. Wind Loads for Structural Design
  - 3.1 Wind Statistics
  - 3.2 Joint Probability of Wind Speeds and Directions
  - 3.3 Upcrossing method to Determine Design Winds
  - 3.4 Mean Wind Speeds at Deck Height
  - 3.5 Transverse Wind Loads as a Function of Annual Probability

## TABLES

- Table 1: Estimated static lateral force coefficient,  $C_x$ , for I-40 Bridge
- Table 2: Dynamic properties and wind conditions considered for Maysville Bridge
- Table 3: Dynamic properties and wind conditions considered for I-40 Bridge
- Table 4: Base transverse loads as a function of annual probability - Maysville Bridge
- Table 5: Base transverse loads as a function of annual probability - I-40 Bridge

## FIGURES

- Figure 1: Maysville Bridge (steel alternate) over Ohio River near Maysville, Kentucky
- Figure 2: I-40 Bridge over Mississippi River on Interstate 40 at Memphis, Tennessee
- Figure 3: Definition of wind angle of attack and static force coefficient
- Figure 4: 1:40 scale sectional model of Maysville Bridge
- Figure 5: Measured static lateral force coefficient,  $C_x$ , for Maysville Bridge
- Figure 6: 1:1500 scale topographic model for Maysville Bridge
- Figure 7: 1:150 scale aeroelastic model of Maysville Bridge
- Figure 8: Definition of base loads for Maysville Bridge
- Figure 9: Definition of base loads for I-40 Bridge
- Figure 10: Base transverse loads as a function of wind speed - Maysville Bridge
- Figure 11: Base transverse loads as a function of wind speed - I-40 Bridge
- Figure 12: Return period wind speed for Maysville Bridge
- Figure 13: Return period wind speed for I-40 Bridge
- Figure 14: Base transverse loads as a function of annual probability - Maysville Bridge
- Figure 15: Base transverse loads as a function of annual probability - I-40 Bridge

## 1. INTRODUCTION

Rowan Williams Davies & Irwin (RWDI) Inc. was retained by Imbsen & Associates, to perform wind loading analysis for the Maysville Bridge (steel alternate design) over Ohio River near Maysville, Kentucky, and the I-40 Bridge over Mississippi River at Memphis, Tennessee, as design examples for the research project NCHRP 12-48 (Design of Highway Bridges for Extreme Events).

The wind loading analysis included:

- wind data analysis for the bridge sites;
- transverse wind loads at the base of the bridge piers as a function of annual probability.

RWDI performed detailed wind tunnel studies for the Maysville Bridge during its design stage<sup>1</sup>, including 1:40 scale sectional model tests, 1:1500 scale topographic model tests, and 1:150 scale aeroelastic model tests. These data were used for the present probability analysis. For the I-40 Bridge, the historic wind data at Memphis were analysed to obtain the wind speeds versus return period at the bridge site. Since no wind tunnel test data were available, the wind loads on the I-40 bridge were estimated using analytical procedures.

The methodology and input data for the analysis are presented in this report.

## 2. DETERMINATION OF TRANSVERSE WIND LOADS ON BRIDGES

Many aspects have to be examined for the wind-resistant design of a long-span bridge, including its aerodynamic stability and wind loading. In this report, only the transverse wind loading will be discussed. Transverse wind loads are those normal to the bridge span in a horizontal direction.

The transverse wind loading consists of three components: the mean loads due to mean wind pressure; the background fluctuating loads due to wind turbulence; and the inertial loads due to wind-induced bridge motions. The mean loads per unit length of span can be expressed in terms of static force coefficients, as follows:

$$P = \frac{1}{2} \rho U^2 B C_x \quad (1)$$

where  $\rho$  = air density;  $U$  = mean wind speed;  $B$  = typical dimension of the bridge; and  $C_x$  = transverse force coefficient (drag coefficient) which can be determined by wind tunnel tests. Wind

<sup>1</sup>Final Report: Wind Engineering Studies for Ohio River Bridge at Maysville, Kentucky (Steel Alternate), *RWDI Report #92-270F*, June 19, 1995



turbulence or gustiness causes fluctuations in wind loading about the mean. These background fluctuating loads are complex since wind gusts are not well correlated along the span or even over the width of the deck. A practical approach to deal with the fluctuating loads is by applying a gust factor on the mean loads. If the fluctuating loads are mainly due to approaching wind turbulence, the gust factor can be estimated for a given bridge based on the knowledge about the turbulence intensity and the turbulence length scale at the site. An important effect of fluctuating wind loads is to induce structural motions, which in turn create inertial loads. The bridge response due to these random fluctuating wind loads is often referred to as the buffeting response. If the buffeting response, in terms of the acceleration of the bridge motion  $\ddot{\delta}$ , can be determined, the inertial loads can be calculated by multiplying the acceleration by the structural mass.

The buffeting response increases with increasing wind speed and also varies with wind direction. For a completed bridge, the worst wind direction is generally normal to the bridge span, although this may not apply in complex terrains. For a bridge during construction, the worst wind direction for some bridge components is often not normal to the bridge span.

Due to the complex interaction of the wind and the bridge span; a precise estimate of buffeting responses can only be made with the aid of wind tunnel tests. There are two types of wind tunnel tests which have been widely used in engineering practice; sectional model tests and full aeroelastic model tests. A sectional model is basically a two dimensional aerodynamic model, from which various aerodynamic parameters, such as aerodynamic force coefficients and aerodynamic derivatives, can be measured. Normally, the results from the sectional model tests have to be combined with an analytical method to obtain the full three-dimensional bridge response<sup>2</sup> Full aeroelastic model tests provide an opportunity to directly measure the three-dimensional bridge responses in strong winds without the aid of analytical approaches. However, the design and construction of an aeroelastic model are much more complicated than a sectional model.

In the following two sections, quasi-static theory based on sectional model tests (or estimated force coefficients) and aeroelastic model tests will be introduced. These two approaches were used for the prediction of the wind loads on the Maysville Bridge and the I-40 Bridge. The two study bridges are illustrated in Figure 1 and Figure 2, respectively.

For the Maysville Bridge, both sectional model and full aeroelastic model tests were conducted. The aeroelastic model tests provided wind-induced responses as a function of wind speed and wind direction. These include the overturning moment at the base of the tower and the deflections of the deck at the mid-span. With the aid of sectional model test results, the wind load distributions over the entire structure could be examined. For the case of the I-40 bridge, where no wind tunnel tests

<sup>2</sup>Irwin, P.A., "Wind tunnel and analytical investigations of the response of Lions' Gate Bridge to a turbulent wind", Nat. Res. Council of Canada, NAE report LTR-LA-210, 1977

were conducted, some well-recognized technical data, such as ESDU<sup>3</sup>, were used, together with RWDI's experience, to estimate the aerodynamic force coefficients. The buffeting response was then calculated based on quasi-static theory.

## 2.1 Determination of Buffeting Response Using Quasi-Static Theory

The wind force affecting the bridge per unit length of the deck at a given instant may be written as

$$P = \frac{1}{2} \rho V^2 B \left( C_{x0} + \frac{dC_x}{d\alpha} \alpha \right) \quad (2)$$

where  $\rho$  = air density;  $V$  = total wind velocity relative to the moving deck;  $B$  = typical dimension of the section (normally taken as depth of the section for lateral force);  $C_x$  = the transverse wind force coefficient;  $C_{x0}$  = the value of  $C_x$  at zero angle of attack;  $\alpha$  = angle of attack.  $C_x$  can be determined from sectional model tests. The definition of wind angle of attack and forces is given in Figure 3.

For the Maysville Bridge, a 1:40 scale sectional model of the bridge deck was tested in RWDI's 8ft×7ft wind tunnel, as shown in Figure 4. Figure 5 presents the measured static lateral force coefficient,  $C_x$ . For the I-40 Bridge, where no wind tunnel data was available, the lateral force coefficients were estimated for each main structural member. The estimated values are given in Table 1.

The total velocity squared may be expressed as

$$V^2 = (U + u - \dot{\delta})^2 + w^2 = U^2 + 2U(u - \dot{\delta}) \quad (3)$$

for small  $(u - \dot{\delta})$  and  $w$ , where  $\dot{\delta}$  is the sway velocity of the structure and  $u$  and  $w$  are the longitudinal and vertical turbulence velocities.

The angle of attack, if it is small, may be written as

$$\alpha = \frac{w}{(U + u - \dot{\delta})} \approx \frac{w}{U} \quad (4)$$

Therefore, the transverse force expression (2) can be written

<sup>3</sup>Engineering Sciences, Characteristics of Atmospheric Turbulence Data Unit Near the Ground: Part III, Variations in Space and Time for Strong Winds, *Engineering Sciences Data Item Number 750001*, London, England, 1993.

$$P = \bar{P} + p = \frac{1}{2} \rho U^2 B C_{x0} + \rho U(u - \dot{\delta}) B C_{x0} + \frac{1}{2} \rho U w B \frac{dC_x}{d\alpha} + \dots \quad (5)$$

As  $u$ ,  $w$  and  $\dot{\delta}$  are relatively small, their higher order terms have been ignored in this expression. The static component,  $\bar{P}$ , produces the mean response (e.g., mean deflections and mean loads) and the dynamic component,  $p$ , is responsible for the buffeting-induced dynamic response. The dynamic component (or wind fluctuating force) per unit length of the span is

$$p = \rho U(u - \dot{\delta}) B C_{x0} + \frac{1}{2} \rho U w B \frac{dC_x}{d\alpha}$$

The general form of the equation of motion of a bridge can be deduced from Lagrange's equation and may be written

$$\ddot{q}_j + 2\zeta_j \omega_j \dot{q}_j + \omega_j^2 q_j = \frac{F_j}{M_j} \quad (7)$$

where  $q_j$  = generalized coordinate for the  $j$ -th mode;  $\omega_j$  = circular frequency for the  $j$ -th mode;  $\zeta_j$  = damping ratio for the  $j$ -th mode;  $M_j$  = generalized mass of the  $j$ -th mode;  $F_j$  = generalized force of the  $j$ -th mode.

Substituting Equation (6) for the transverse force into Equation (7), but replacing  $\dot{\delta}$  by  $\phi_j \dot{q}_j$ , where  $\phi$  is the modal deflection shape, we obtain

$$\ddot{q}_j + 2\zeta_j \omega_j \dot{q}_j + \omega_j^2 q_j = \frac{\int_0^L \left( \rho U(u - \phi_j \dot{q}_j) B C_{x0} + \frac{1}{2} \rho U w B \frac{dC_x}{d\alpha} \right) \phi_j dy}{M_j}$$

If the mean wind speed,  $U$ , and the density,  $\rho$ , are constant along the span, Equation (8) can be rewritten as

$$\ddot{q}_j + 2\zeta_j \omega_j \dot{q}_j + \omega_j^2 q_j = \frac{\rho U \int_0^L \left( (u B C_{x0} + \frac{1}{2} w B \frac{dC_x}{d\alpha}) \phi_j dy \right)}{M_j} \quad (9)$$

where  $\zeta_{jT}$  is the total damping ratio for the  $j$ -th mode, including structural damping and aerodynamic damping.

$$\zeta_{jT} = \zeta_j + \zeta_{ja} = \zeta_j + \frac{\rho U \int_0^L \phi_j^2 B C_{x0} dy}{2 \omega M_j} \quad (10)$$

For light damping and using the fact that the correlation of gusts at different points on the span falls off quite quickly with span wise separation, the variance of the transverse response can be obtained from Equation (9) and expressed in the following form and expressed in the following form.

$$\begin{aligned} \sigma_{qj}^2 = & \frac{B^2}{16\pi^4} \left( \frac{\rho B^2}{m_{eff}} \right)^2 \left( \frac{U}{n_j B} \right)^4 \frac{\pi}{4\zeta_{jT}} I_u^2 C_{x0,eff}^2 \bar{S}_u(n_j) \bar{C}_{luu}(n_j) F_{Juu}(n_j) \\ & + \frac{1}{4} I_w^2 \left( \frac{dC_x}{d\alpha} \right)_{eff}^2 \bar{S}_w(n_j) \bar{C}_{lww}(n_j) F_{Jww}(n_j) + I_u I_w \left( C_{x0} \frac{dC_x}{d\alpha} \right)_{eff} \sqrt{\bar{S}_u(n_j) \bar{S}_w(n_j)} \bar{C}_{luw}(n_j) F_{Juw}(n_j) \end{aligned}$$

where

$$\text{Effective mass:} \quad m_{eff} \equiv \frac{M_j}{L} \quad (12)$$

Effective force coefficients:

$$C_{x0,eff} = \sqrt{\frac{\int_0^L C_{x0}^2 \phi_j^2 dy}{L}} \quad ; \quad \left( \frac{dC_x}{d\alpha} \right)_{eff} = \sqrt{\int_0^L \left( \frac{dC_x}{d\alpha} \right)^2 \phi_j^2 dy}$$

$$\left( C_{x0} \frac{dC_x}{d\alpha} \right)_{eff} = \frac{\int_0^L C_{x0} \frac{dC_x}{d\alpha} \phi_j^2 dy}{L}$$

Normalized wind turbulence spectra:

$$\bar{S}_u(n) = \frac{n S_u(n)}{\sigma_u^2} \quad ; \quad \bar{S}_w(n) = \frac{n S_w(n)}{\sigma_w^2}$$

Normalized cross spectra of wind turbulence:

$$\bar{C}_{uu}(n) = \frac{3.774 \left( \frac{L_u^y}{L} \right)}{\sqrt{1 + 70.78 \left( \frac{2nL_u^y}{U} \right)^2}} \quad \bar{C}_{vv}(n) = \frac{1425 \left( \frac{L_v^y}{L} \right) \left( \frac{2nL_v^y}{U} \right)^2}{\sqrt{1 + 70.78 \left( \frac{2nL_v^y}{U} \right)^2 \left( 1 + 188.8 \left( \frac{2nL_v^y}{U} \right)^2 \right)}} \quad (15)$$

$$\bar{C}_{uv}(n) = - \frac{1}{\frac{0.747L}{\sqrt{L_u^y L_v^y}} \sqrt{1 + 283.1 \left( \frac{n\sqrt{L_u^y L_v^y}}{U} \right)^2}}$$

$F_{Juu}$ ,  $F_{Jvv}$  and  $F_{Juv}$  are the correction factors for correlation length of wind turbulence.

The peak response can be determined by applying a peak factor to the estimated RMS (root-mean-square) response. A typical value for peak factors is between 3.5 and 4.0.

The dynamic properties and wind conditions considered in the present study are listed in Table 2 and Table 3 for Maysville Bridge and I-40 Bridge, respectively.

## 2.2 Determination of Buffeting Response Using Full Aeroelastic Model Tests.

Aeroelastic model tests require a larger wind tunnel than for sectional model tests. The boundary layer wind tunnel used for the aeroelastic model tests of the Maysville Bridge was RWDI's 16ftx8ft wind tunnel. With this wind tunnel, the length scale of the aeroelastic bridge model was set at 1:150.

### *Simulation of the Natural Wind*

In aeroelastic model tests, the natural wind has to be simulated. Due to the complexity of the topography around the proposed Maysville bridge site, the effects of these surroundings on the wind flow characteristics at the site were examined using a 1:1500 scale topographic model before the aeroelastic model tests. Figure 6 shows the topographic model in RWDI's 16ftx8ft boundary layer wind tunnel.

In the topographic model tests, the mean wind velocity and turbulence parameters were measured for 16 equally spaced wind directions. The turbulence intensities at the deck height were measured

to be about 0.20 in the longitudinal wind direction and about 0.09 in the vertical direction for wind approaching along the river. For wind not approaching the bridge site along the river, the longitudinal turbulence intensity was in the range of 0.25 to 0.3 and vertical turbulence intensity was in the range of 0.09 to 0.14.

The topographic model results were used to establish appropriate simulations of the natural wind at the site for the 1:150 scale aeroelastic model tests.

In the aeroelastic model tests, the mean velocity profile and the turbulence intensity of the natural wind were simulated with a roughened floor and specially designed turbulent generators at the upwind end of the working section. The impact of surroundings on wind flow at the site was also simulated by modelling local surrounding topography. It should be noted that, although the mean velocity profile and the turbulence intensity can be well simulated, the simulation of the wind turbulence integral scale in the wind tunnel is more approximate because the natural turbulence scales vary over quite large ranges. Due to physical constraints, the wind tunnel tends generally to give a value corresponding to the low end of the range seen at full scale. The sensitivity of the wind-induced response to possible variations in integral scale therefore needs some consideration. A theoretical buffeting analysis is therefore used to assess the impact of varying turbulence length scale.

The bridge model was mounted on a rigid turntable in the wind tunnel. This allowed any wind direction to be simulated by rotating the model to the appropriate angle in the wind tunnel.

### *Simulation of the Structure*

An analysis of the phenomena governing the wind responses of suspended bridges indicates that, in order for an aeroelastic model to be dynamically similar to the prototype, the following non-dimensional parameters should be the same for the model and the prototype bridges:

Froude Number	(ratio of fluid inertia force to vertical force due to gravity);
Cauchy Number	(ratio of elastic force to fluid inertia force);
Reynolds Number	(ratio of fluid inertial force to fluid viscous force);
Density Parameter	(ratio of inertia force of the structure to that of the flow); and
Damping Ratio	(ratio of the damping to the critical damping value).

For an aeroelastic model test, it is usually not practical, nor is it necessary, to obtain Reynolds number similarity except for an object with circular or rounded edges. For sharp-edged structures such as the bridge decks of the Maysville bridge, the effects of the Reynolds number on the wind-induced responses are typically very small over a wide range. Therefore, Reynolds number scaling

can be relaxed for the design of the deck and the towers. To obtain the correct cable drag, because of a change in cable drag coefficient induced by the small model Reynolds number, the model cable diameters have to be adjusted to compensate for the Reynolds number mismatch. Also for smaller elements such as railings, it is necessary to reduce their number and increase their size so as to avoid low Reynolds number effects.

The aeroelastic model of the Maysville bridge was composed of a spine and shell system, to provide the required structural stiffness, the inertial properties, and the geometric shape. Based on matching of the above non-dimensional parameters, the ratios of the model physical properties to the corresponding full scale values can be readily deduced. These are summarized in Table 1. For example:

the ratio for model force to full scale force is the cube of the length scale;  
the ratio of model velocity to full scale velocity is the square root of the length scale; and  
the ratio of model time to full scale time is also the square root of the length scale.

### *Instrumentation and Model Set Up*

The aeroelastic model of the Maysville bridge was instrumented with strain gauges, accelerometers and displacement transducers for the measurement of bending moments, shear forces, accelerations and displacements at various points on the structure.

The displacement transducers were divided into several sets. Each set measured three components of displacement at a single location: vertical, lateral, and torsional. By installing these sets at different locations along the span, the deck displacements were measured simultaneously at the different locations (e.g., mid-span, quarter-span, etc.).

Strain gauges were used to measure the wind-induced loads on the tower columns and the tower base. By calibration, the strain gauges attached to the tower spine system would provide the bending moments at each strain gauge location. A combination of two levels of strain gauges provided the shear forces and the overturning moments at the base. Accelerometers were installed on the top of the bridge tower to measure the wind-induced accelerations.

The strain gauge, accelerometer and displacement transducer signals were sampled at a chosen rate for a given time duration at full scale, such as one hour. A statistical analysis was then followed to obtain the predicted wind-induced response.

The aeroelastic model of the Maysville Bridge is shown in Figure 7.

### 3. WIND LOADS FOR STRUCTURAL DESIGN

From the analysis and testing described in Section 1, the lateral wind loads for the Maysville Bridge and the I-40 Bridge could be determined as a function of wind speed and wind direction. Figures 10 and 11 show the predicted transverse peak base loads at the worst wind direction as a function of wind speed for the Maysville bridge and the I-40 bridge. The definitions of these base loads are illustrated in Figure 8 and Figure 9 for the Maysville Bridge and the I-40 Bridge, respectively.

For structural design purposes, these results need to be combined with statistical wind data at the site to present the peak wind loads as a function of return period. Since long span bridges are important structures, a 100-year return period is normally chosen for structural design wind loads.

#### 3.1 Wind Statistics

To determine the design wind speeds for the bridge, the following two steps were involved:

- (i) Determine the joint probability of wind speed and direction for the site based on available meteorological data. The joint probability was expressed in the form of a mathematical model fitted to the meteorological data.
- (ii) Use the mathematical model from (i) to evaluate the wind speed as a function of return period and also to evaluate the component of wind velocity normal to the span as a function of return period. A procedure called "Upcrossing Analysis" was used in this second step.

In addition, extreme value analyses using the Gumbel's moment fitting procedure and a least squared fitting procedure were undertaken for comparison, using the local meteorological data.

For the Maysville bridge, the wind data recorded at the three closest weather stations were used for the first step, which included:

1. the Great Cincinnati Airport in Covington, Kentucky, located 45 miles northwest of the bridge site;
2. the Blue Grass Airport in Lexington, Kentucky, located 55 miles southwest of the site; and
3. the Tri-State Airport in Huntington, West Virginia, located 70 miles east-southeast of the site.

For the I-40 bridge, the wind data recorded at the Memphis International Airport, Tennessee, were used.



### 3.2 Joint Probability of Wind Speeds and Directions

A mathematical model of the joint probability of mean hourly wind speed and direction was fitted to the meteorological wind data and the Weibull distribution was assumed for this fitting. The Weibull distribution expresses the probability of the wind speed at gradient height exceeding a value  $U_G$  as

$$P_{\theta}(U_G) = A_{\theta} \exp \left[ - \left( \frac{U_G}{C_{\theta}} \right)^{K_{\theta}} \right] \quad (16)$$

where  $P_{\theta}$  = probability of exceeding the gradient wind speed  $U_G$  in the angle sector  $\theta$   
 $\theta$  = centre angle of an angle sector, measured clockwise from true north  
 $U_G$  = wind speed at gradient height  
 $A_{\theta}, C_{\theta}, K_{\theta}$  = coefficients selected to give best fit to the data

Note that  $A_{\theta}$  is the fraction of time the wind blows from within the angle sector  $\theta$ . The size of angle sectors used in the analysis was 10 degrees. To provide additional flexibility in curve fitting, two curves of the Weibull form were fitted, one to lower velocities and one to higher velocities, a blending expression being used to provide a smooth transition.

The gradient wind speed  $U_G$  is well above the earth's surface, sufficiently high to be essentially free of surface roughness effects. The height used for determining gradient speed was 2000 ft. Since the anemometer is near ground level at the bottom of the planetary boundary layer, it is affected by ground roughness. The ground roughness effects were assessed using the methods documented in ESDU combined with information on local terrain roughness gathered from the topographic maps. Factors were developed to convert the anemometer records to wind speeds at gradient height.

From the above probability distribution, Equation (16), the overall probability of wind speed is obtained by summing over all wind directions

$$P(U_G) = \sum_{\theta} P_{\theta}(U_G) \quad (17)$$

### 3.3 Upcrossing Method to Determine Design Winds

Using probability theory (Rice<sup>4</sup>), it can be shown that the return period years,  $R$ , of a given gradient wind speed,  $U_G$ , is related to  $P(U_G)$  by

$$R = \frac{|\dot{U}_G|}{2} \frac{dP(U_G)}{dU_G}$$

where  $|\dot{U}_G|$  is the average of the absolute rate of change of  $U_G$  with time.

Equation (18) was used to determine the return periods for a series of selected gradient wind speeds. The wind speed corresponding to a selected return period, e.g., 100 years, could then be determined by interpolation. This method is called the Upcrossing Method.

For the consideration of transverse buffeting response of a completed bridge, it is possible to account for the effects of wind directionality by using an effective wind speed weighted by the cosine of the wind direction angle relative to the normal to the span<sup>5</sup>. Therefore, it is of interest to evaluate this effective normal wind speed component as a function of return period.

It can be shown<sup>6,7</sup> that if  $U_B$  denotes the wind velocity on the boundary of interest (in this case, it is the velocity corresponding to a given level of load effects), then the return period  $R$  is given by

$$R = \left[ \sqrt{1 + \left( \frac{|\dot{\theta}_B|}{|\dot{U}_B|} \frac{dU_B}{d\theta} \right)^2} \right]^{-1}$$

where  $|\dot{U}_B|$  and  $|\dot{\theta}_B|$  are the mean absolute rates of changes of wind speed and wind direction, respectively which are further statistical parameters that are determined from the meteorological data.

<sup>4</sup>Rice, S.O., "Mathematical Analysis of Random Noise", *The Bell System Technical Journal*, Vol. 23, 1944.

<sup>5</sup>Xie, J, et al, "Buffeting Analysis of Long Span Bridges to Turbulent Wind with Yaw Angle", *Journal of Wind Engineering and Industrial Aerodynamics*, Vol.37, 1991

<sup>6</sup>Lepage, M.F., and Irwin, P.A., "A Technique for Combining Historic Wind Data with Wind Loads", *Proc. 5th U.S. National Conference on Wind Engineering*, Lubbock, Texas, 1985.

<sup>7</sup>Irwin, P.A., "Prediction and Control of the Wind Response of Long Span Bridges with Plate Girder Decks", *Proc. Structures Congress '87/ST Div/ASCE*, Orlando, Florida, August 17-20, 1987.

### **3.4 Mean Wind Speeds at Deck Height**

To convert the wind data to the bridge deck height, the following factors have been used:

- (1) *Factors relating the recorded wind speed to the wind speed at gradient height*  
These factors were based on the topographic information around the meteorological station
- (2) *Factors relating the gradient wind speed to the wind speed at deck level*  
These factors were based on the topographic information around the bridge site.

To be consistent with the ASCE-7 Standard, the predicted wind speed as a function of return period has been re-scaled to force the 50-year wind speed at 33ft height in a standard open terrain to be 70 mph fastest mile for both the Maysville bridge and I-40 bridge. To convert a fastest mile speed to the corresponding mean hourly speed, a reduction factor of 1.27 was used. Figures 12 and 13 present the estimated mean wind speeds at the bridge deck levels as a function of return periods for the Maysville Bridge and the I-40 Bridge, respectively. The longitudinal wind turbulence intensity at the bridge deck level was estimated to be 20% for the Maysville bridge and 16% for the I-40 bridge.

### **3.5 Transverse Wind Loads as a Function of Annual Probability**

Combining the wind response data given in Figures 10 and 11 with the local wind climate data given in Figures 12 and 13, Figures 14 and 15 present the estimated base transverse wind loads as a function of annual probability. For the Maysville bridge, the loads are those acting on the piers at EL. 470ft, as defined in Figure 8. For the I-40 bridge, the loads are those acting on the central pier (Pier B) at EL.172ft, as defined in Figure 9.

The annual probability is defined in the same way as ASCE 7-98. Therefore, an annual probability of 0.02 corresponds to a 50-year return period and 0.01 corresponds to a 100-year return period. Values greater than 1 indicate the number of events per year. Typically, the duration of a strong wind event lasts for about 3 hours.

**Table 1:** Estimated static lateral force coefficient,  $C_x$ , of I-40 Bridge

<b>Structural Members</b>	<b>Estimated force coefficient <math>C_x</math></b>
Top chords of truss	1.9
Bottom chords of truss	1.9
Vertical members of truss	1.9
Diagonal members of truss	1.9
Hangers	1.2
Deck	1.5
Piers	0.8

**Note:**

The given force coefficient,  $C_x$ , was based on the frontal depth (or width) of each member.

**Table 2:** Dynamic properties and wind conditions considered for Maysville Bridge

<b>Mass (slugs/ft)</b>		
Main span deck	$M = 330.8$ slugs/ft	
Tower column upper leg	$M = 458.8$ slugs/ft	
Tower column middle leg	$M = 406.5$ slugs/ft	
Tower column lower leg	$M = 775.8$ to $1462.1$ slugs/ft	
Tower column base	$M = 3897.6$ slugs/ft	
Tower upper strut	$M = 130.5$ slugs/ft	
Tower lower strut	$M = 130.5$ slugs/ft	
<b>Modes of Vibration</b>		
1 <sup>st</sup> lateral mode	$f = 0.5103$ Hz	$\zeta = 1.0\%$
1 <sup>st</sup> vertical mode	$f = 0.3368$ Hz	$\zeta = 1.0\%$
2 <sup>nd</sup> vertical mode	$f = 0.4287$ Hz	$\zeta = 1.0\%$
1 <sup>st</sup> torsional mode	$f = 0.6123$ Hz	$\zeta = 1.0\%$
<b>Wind Conditions</b>		
10-year return period	$U = 56$ mph	$I_u = 20\%$ ; $I_w = 9\%$
50-year return period	$U = 61$ mph	$I_u = 20\%$ ; $I_w = 9\%$
100-year return period	$U = 64$ mph	$I_u = 20\%$ ; $I_w = 9\%$
<b>Wind Profiles</b>		
Logarithm profile of mean wind speed	$\alpha \approx 0.176$	
Logarithm profile of longitudinal turbulence	$\alpha_T \approx -0.170$	

**Note:**

$M =$  mass per unit length

$f =$  natural frequency

$\zeta =$  structural damping ratio

$U =$  mean hourly wind speed at deck level (i.e., at El.576.5 ft). The water level is assumed to be at El.485.5 ft.

$I_u =$  longitudinal turbulence intensity at deck level

$I_w =$  vertical turbulence intensity at deck level

**Table 3:** Dynamic properties and wind conditions considered for I-40 Bridge

<b>Modes of Vibration</b>		
1 <sup>st</sup> lateral mode (asymmetrical)	$f = 0.2874$ Hz	$\zeta = 1.0\%$
2 <sup>nd</sup> lateral mode (symmetrical)	$f = 0.3356$ Hz	$\zeta = 1.0\%$
<b>Wind Speed and Turbulence Intensity at Deck Level</b>		
10-year return period	$U = 59$ mph	$I_u = 16\%$ ; $I_w = 8\%$
50-year return period	$U = 66$ mph	$I_u = 16\%$ ; $I_w = 8\%$
100-year return period	$U = 71$ mph	$I_u = 16\%$ ; $I_w = 8\%$
<b>Wind Profiles</b>		
Logarithm profile of mean wind speed	$\alpha = 0.14$	
Logarithm profile of longitudinal turbulence	$\alpha_T = -0.17$	

**Note:**

$f =$  natural frequency

$\zeta =$  structural damping ratio

$U =$  mean hourly wind speed at deck level (i.e., at El.304.6 ft) . The water level is assumed to be at El.183.2 ft.

$I_u =$  longitudinal turbulence intensity at deck level

$I_w =$  vertical turbulence intensity at deck level

The structural mass was not considered for this study case, since the mass tends to be less sensitive to the wind-induced lateral forces.

**Table 4: Base transverse loads as a function of annual probability - Maysville Bridge**

Annual Probability	Shear (kips)	Moment (kips-ft)	Annual Probability	Shear (kips)	Moment (kips-ft)	Annual Probability	Shear (kips)	Moment (kips-ft)
9.48842	2.059E+02	3.559E+04	0.34011	4.058E+02	7.013E+04	0.00749	6.729E+02	1.163E+05
8.14463	2.139E+02	3.697E+04	0.28771	4.170E+02	7.207E+04	0.00613	6.873E+02	1.188E+05
6.98543	2.221E+02	3.838E+04	0.24309	4.284E+02	7.403E+04	0.00501	7.019E+02	1.213E+05
5.98709	2.304E+02	3.981E+04	0.20512	4.399E+02	7.601E+04	0.00409	7.166E+02	1.238E+05
5.12845	2.388E+02	4.127E+04	0.17285	4.515E+02	7.803E+04	0.00334	7.314E+02	1.264E+05
4.39077	2.474E+02	4.276E+04	0.14546	4.633E+02	8.007E+04	0.00271	7.464E+02	1.290E+05
3.75756	2.562E+02	4.427E+04	0.12224	4.753E+02	8.213E+04	0.00220	7.616E+02	1.316E+05
3.21439	2.651E+02	4.581E+04	0.10258	4.874E+02	8.423E+04	0.00178	7.769E+02	1.342E+05
2.74869	2.742E+02	4.738E+04	0.08596	4.997E+02	8.634E+04	0.00144	7.924E+02	1.369E+05
2.34955	2.834E+02	4.897E+04	0.07192	5.121E+02	8.849E+04	0.00116	8.080E+02	1.396E+05
2.00753	2.928E+02	5.059E+04	0.06009	5.247E+02	9.066E+04	0.00094	8.237E+02	1.423E+05
1.71452	3.023E+02	5.223E+04	0.05013	5.374E+02	9.286E+04	0.00075	8.396E+02	1.451E+05
1.46352	3.119E+02	5.390E+04	0.04175	5.502E+02	9.508E+04	0.00061	8.557E+02	1.479E+05
1.24856	3.218E+02	5.560E+04	0.03472	5.633E+02	9.733E+04	0.00048	8.719E+02	1.507E+05
1.06447	3.317E+02	5.733E+04	0.02883	5.764E+02	9.961E+04	0.00039	8.883E+02	1.535E+05
0.90687	3.419E+02	5.908E+04	0.02390	5.898E+02	1.019E+05	0.00031	9.048E+02	1.564E+05
0.77199	3.522E+02	6.085E+04	0.01978	6.033E+02	1.042E+05	0.00025	9.215E+02	1.592E+05
0.65659	3.626E+02	6.266E+04	0.01634	6.169E+02	1.066E+05	0.00020	9.384E+02	1.621E+05
0.55791	3.732E+02	6.449E+04	0.01348	6.307E+02	1.090E+05	0.00015	9.553E+02	1.651E+05
0.47358	3.839E+02	6.634E+04	0.01110	6.446E+02	1.114E+05	0.00012	9.725E+02	1.680E+05
0.40156	3.948E+02	6.822E+04	0.00912	6.587E+02	1.138E+05	0.00010	9.898E+02	1.710E+05

**Note:** The given base shears and base overturning moments are on the Pier at EL.470ft in the transverse direction, as defined in Figure 8. The annual probability is defined in the same way as ASCE 7-98. Therefore, an annual probability of 0.02 corresponds to a 50-year return period and 0.01 corresponds to a 100-year return period. Values greater than 1 indicate the number of events per year.

**Table 5: Base transverse loads as a function of annual probability I-40 Bridge**

Annual Probability	Shear (kips)	Moment (kips-ft)	Annual Probability	Shear (kips)	Moment (kips-ft)	Annual Probability	Shear (kips)	Moment (kips-ft)
9.94559	3.661E+02	8.036E+04	0.05839	9.040E+02	1.984E+05	0.00167	1.681E+03	3.690E+05
8.12100	3.853E+02	8.459E+04	0.04728	9.341E+02	2.051E+05	0.00146	1.722E+03	3.780E+05
6.59270	4.051E+02	8.893E+04	0.03854	9.647E+02	2.118E+05	0.00128	1.763E+03	3.871E+05
5.32191	4.253E+02	9.338E+04	0.03164	9.958E+02	2.186E+05	0.00112	1.805E+03	3.963E+05
4.27285	4.461E+02	9.793E+04	0.02614	1.027E+03	2.256E+05	0.00098	1.848E+03	4.057E+05
3.41295	4.673E+02	1.026E+05	0.02174	1.060E+03	2.326E+05	0.00086	1.891E+03	4.151E+05
2.71294	4.891E+02	1.074E+05	0.01819	1.092E+03	2.398E+05	0.00076	1.934E+03	4.246E+05
2.14688	5.113E+02	1.122E+05	0.01530	1.125E+03	2.470E+05	0.00067	1.978E+03	4.343E+05
1.69209	5.340E+02	1.172E+05	0.01293	1.159E+03	2.544E+05	0.00059	2.023E+03	4.441E+05
1.32893	5.572E+02	1.223E+05	0.01098	1.193E+03	2.619E+05	0.00052	2.068E+03	4.539E+05
1.04062	5.809E+02	1.275E+05	0.00936	1.227E+03	2.695E+05	0.00046	2.113E+03	4.639E+05
0.81297	6.051E+02	1.328E+05	0.00801	1.263E+03	2.772E+05	0.00040	2.159E+03	4.740E+05
0.63409	6.298E+02	1.383E+05	0.00688	1.298E+03	2.850E+05	0.00035	2.205E+03	4.842E+05
0.49416	6.550E+02	1.438E+05	0.00592	1.334E+03	2.929E+05	0.00031	2.252E+03	4.945E+05
0.38512	6.807E+02	1.494E+05	0.00511	1.371E+03	3.009E+05	0.00028	2.300E+03	5.049E+05
0.30042	7.069E+02	1.552E+05	0.00442	1.408E+03	3.091E+05	0.00024	2.348E+03	5.154E+05
0.23478	7.335E+02	1.610E+05	0.00383	1.445E+03	3.173E+05	0.00022	2.396E+03	5.260E+05
0.18399	7.607E+02	1.670E+05	0.00332	1.483E+03	3.256E+05	0.00019	2.445E+03	5.368E+05
0.14472	7.884E+02	1.731E+05	0.00289	1.522E+03	3.341E+05	0.00017	2.494E+03	5.476E+05
0.11436	8.165E+02	1.793E+05	0.00252	1.561E+03	3.427E+05	0.00015	2.544E+03	5.586E+05
0.09084	8.452E+02	1.855E+05	0.00219	1.600E+03	3.513E+05	0.00013	2.595E+03	5.696E+05
0.07260	8.743E+02	1.919E+05	0.00191	1.640E+03	3.601E+05	0.00012	2.646E+03	5.808E+05

**Note:** The given base shears and base overturning moments are on the Pier B at EL.172ft in the transverse direction, as defined in Figure 9. The annual probability is defined in the same way as ASCE 7-98. Therefore, an annual probability of 0.02 corresponds to a 50-year return period and 0.01 corresponds to a 100-year return period. Values greater than 1 indicate the number of events per year.



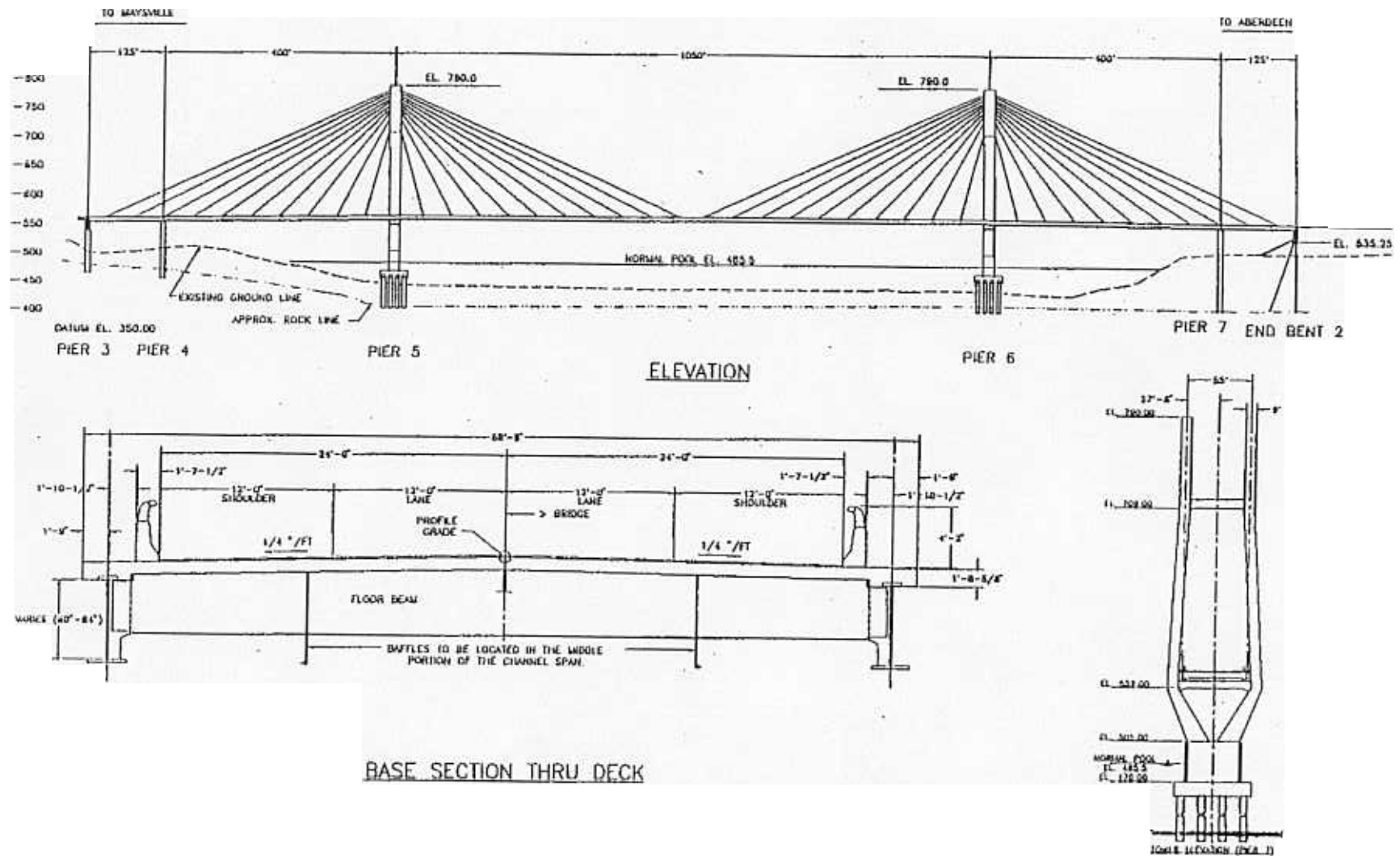


Figure 1: Maysville Bridge (Steel Alternative) over Ohio River near Maysville, Kentucky

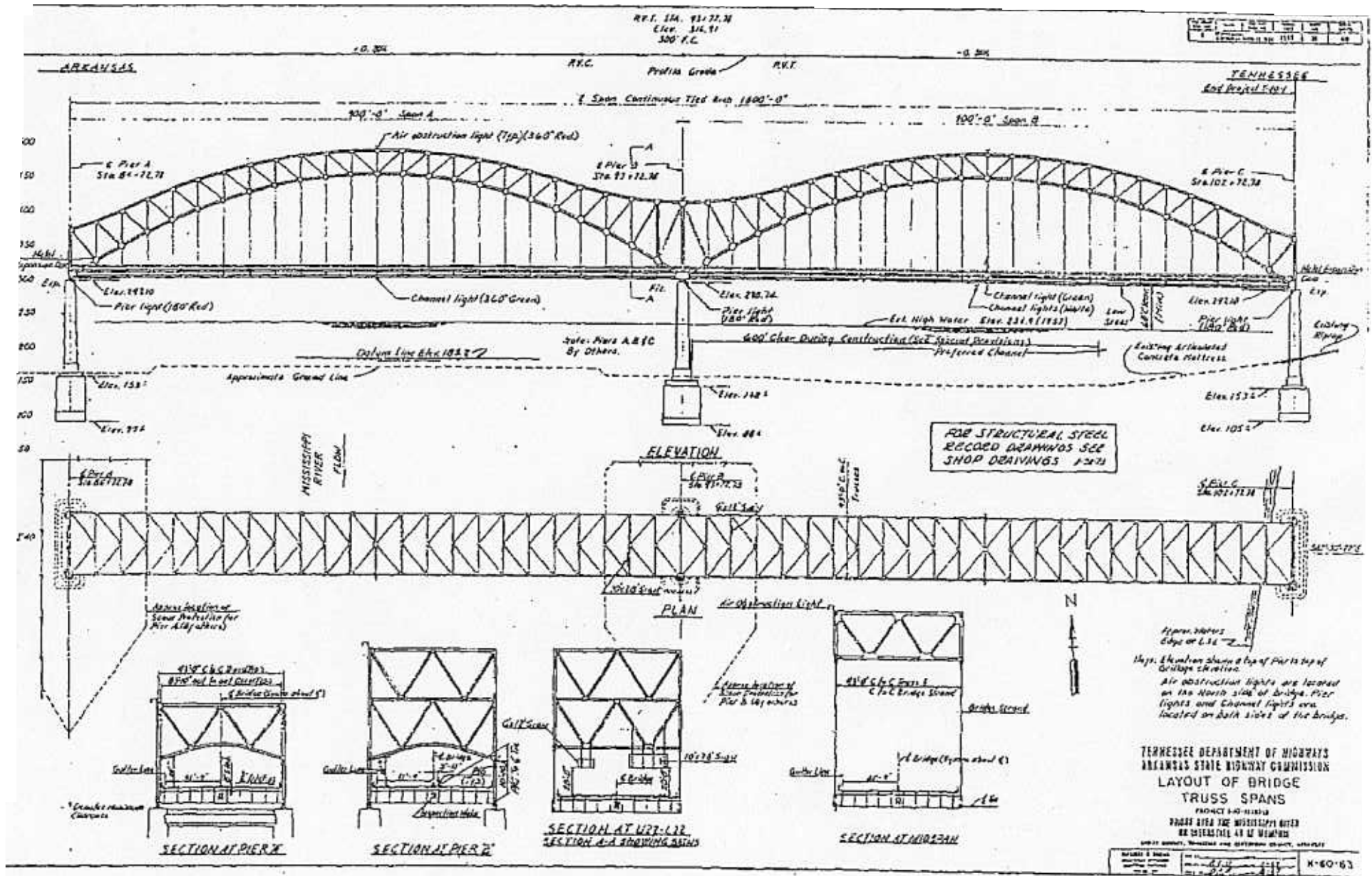
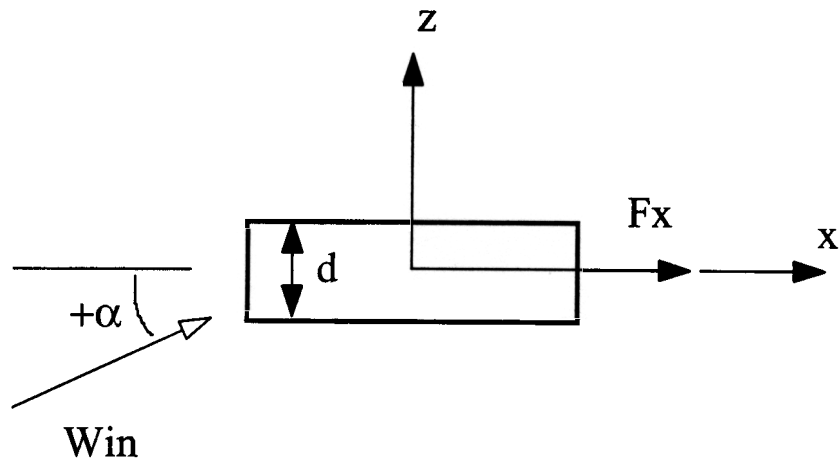


Figure 2: 2-40 Bridge over Mississippi River on Interstate 40 at Memphis, Tennessee

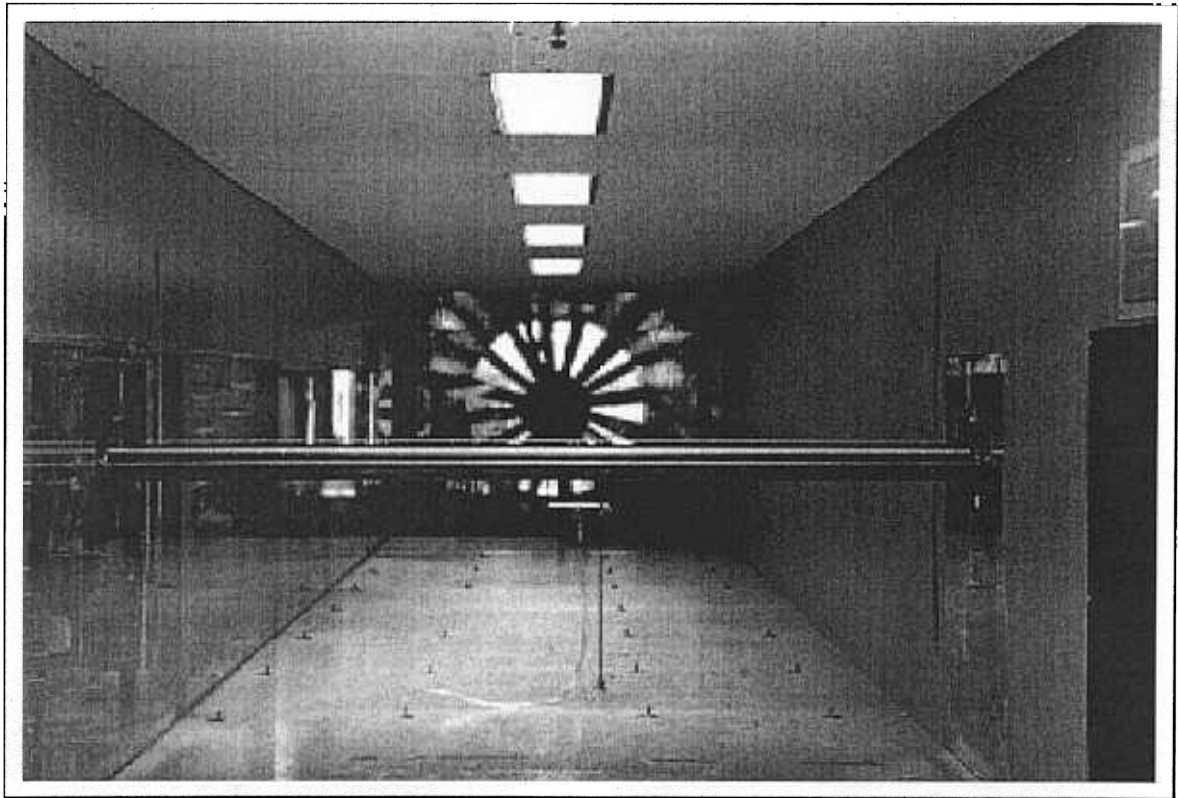


Static lateral force coefficient:

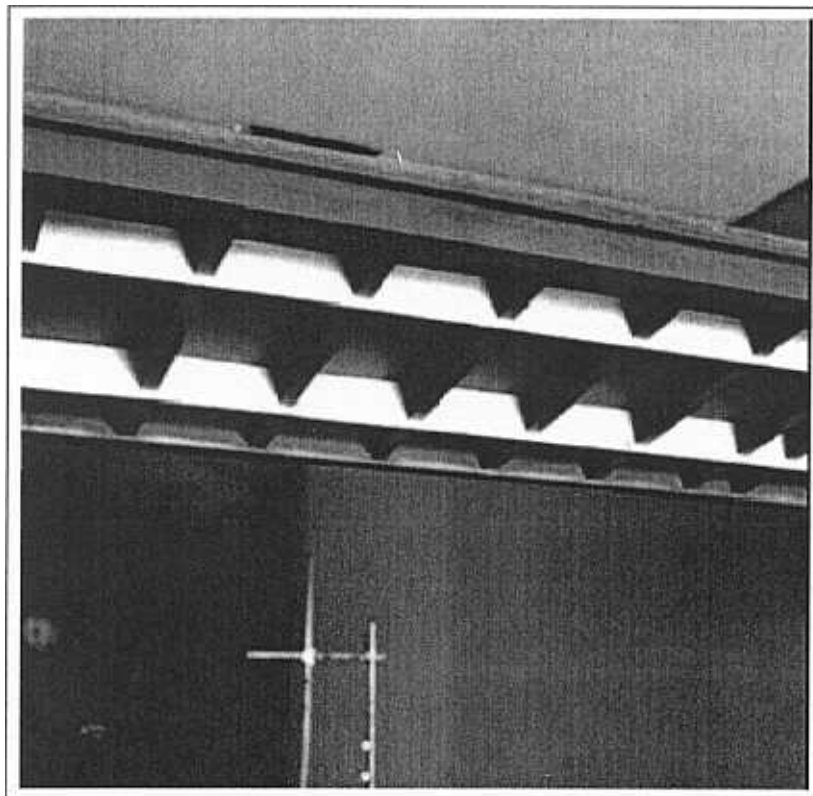
$$C_x = \frac{F_x}{\frac{1}{2}\rho U^2 d}$$

where  $F_x$  = lateral force;  
 $\rho$  = air density;  
 $U$  = wind speed at deck level;  
 $d$  = typical dimension of the deck.

**Figure 3:** Definition of wind angle of attack and static force coefficient

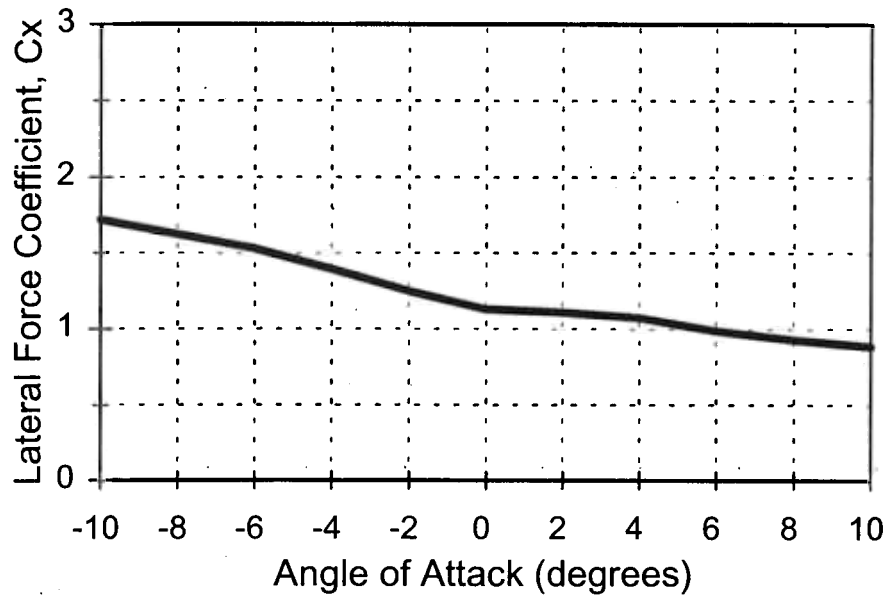


a) view from above



b) view from below (with baffles)

**Figure 4:** 1:40 scale sectional model of Maysville Bridge



The lateral force coefficient,  $C_x$ , is defined as follows:

$$C_x = \frac{F_x}{\frac{1}{2}\rho U^2 d}$$

where  $F_x$  = lateral force;

$\rho$  = air density;

$U$  = wind speed at deck level;

$d$  = typical dimension of the deck, taken as the deck depth ( $d = 9.2$  ft)

**Figure 5:** Measured static lateral force coefficient,  $C_x$ , for Maysville Bridge

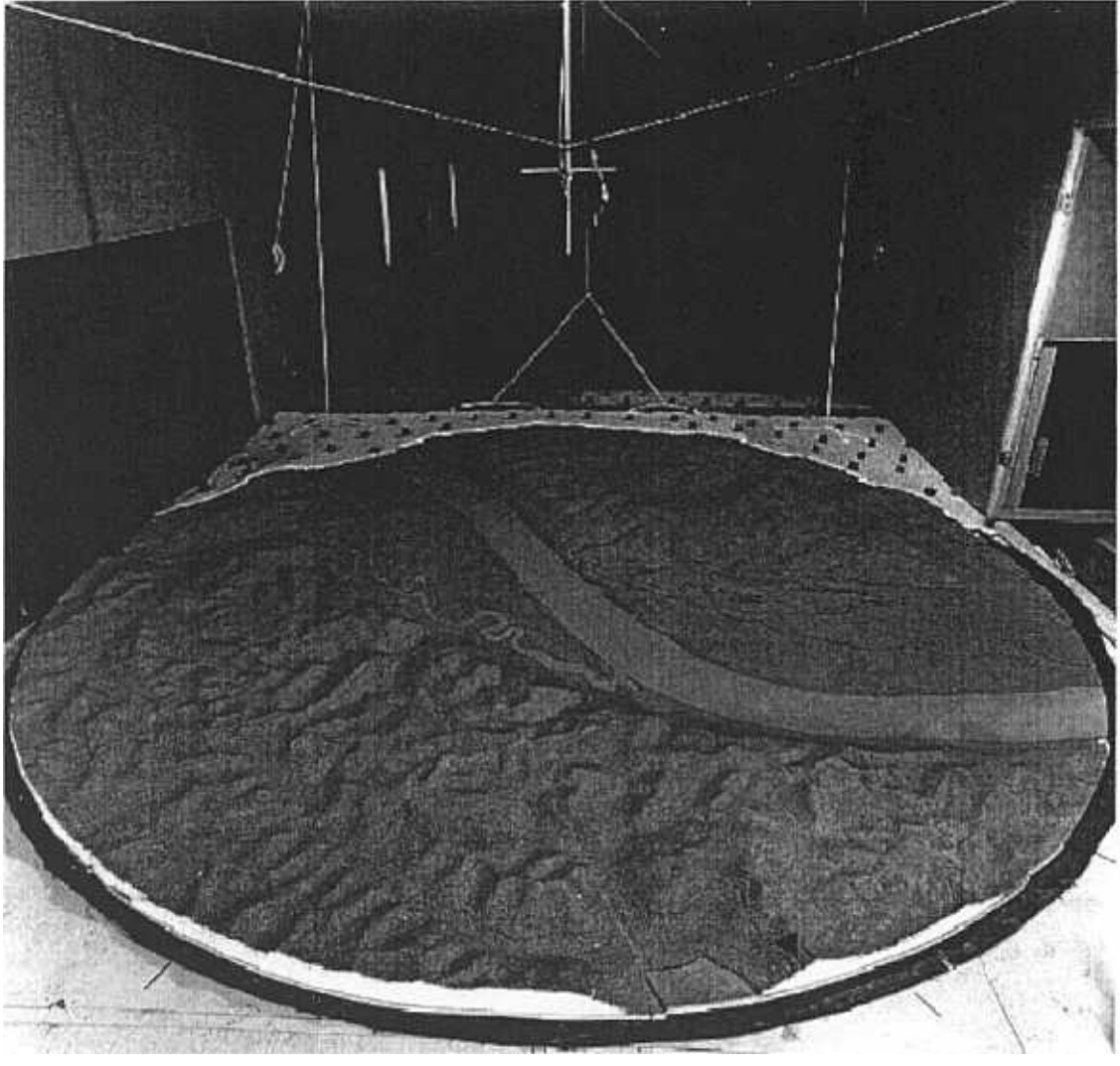


**Figure 6:** 1:1500 scale topographic model for Maysville Bridge

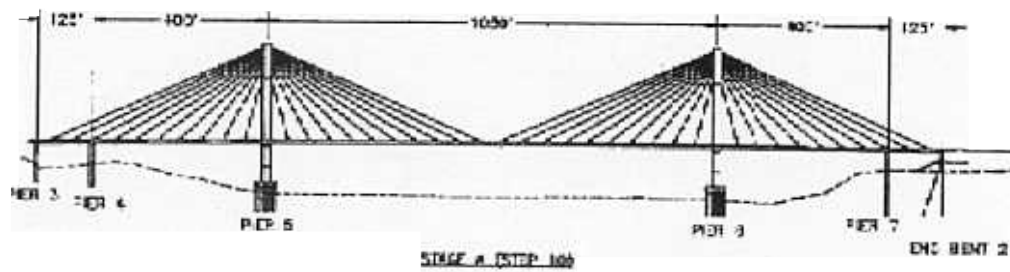
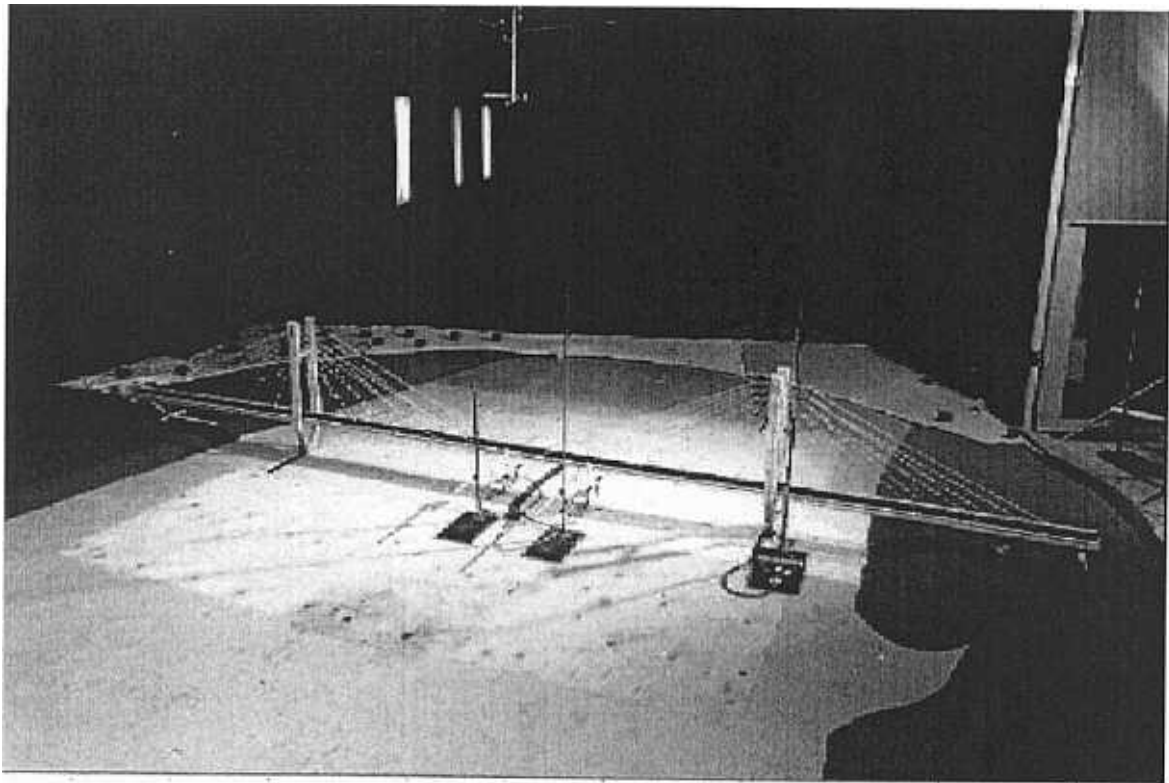


**Figure 7: 1:150 scale aeroelastic model of Maysville Bridge**

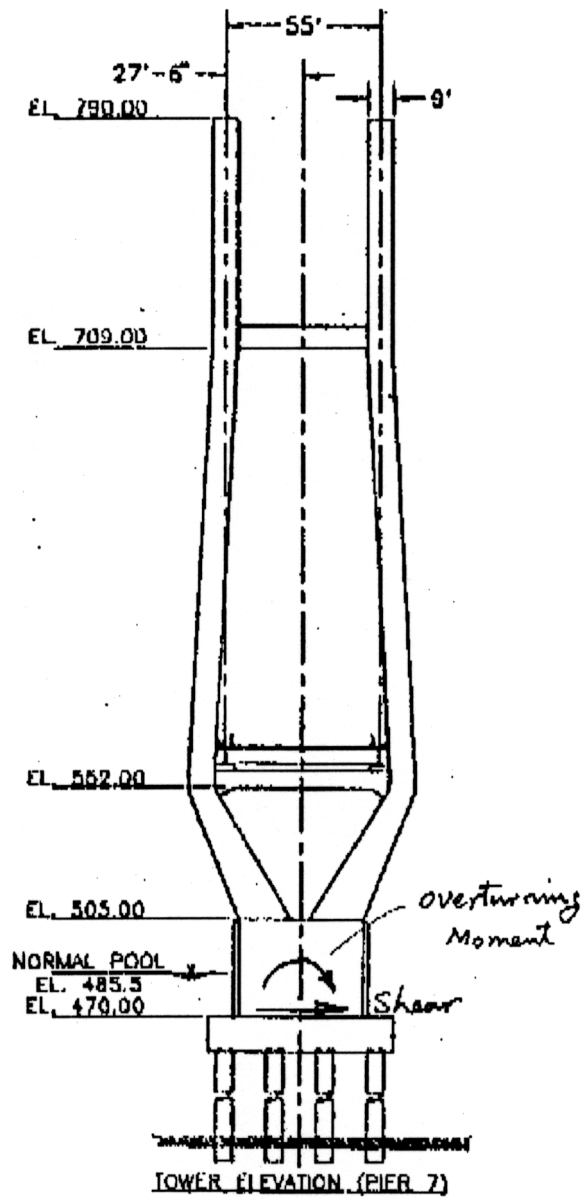


**Figure8:** Definition of base loads for Maysville Bridge



# Pier B

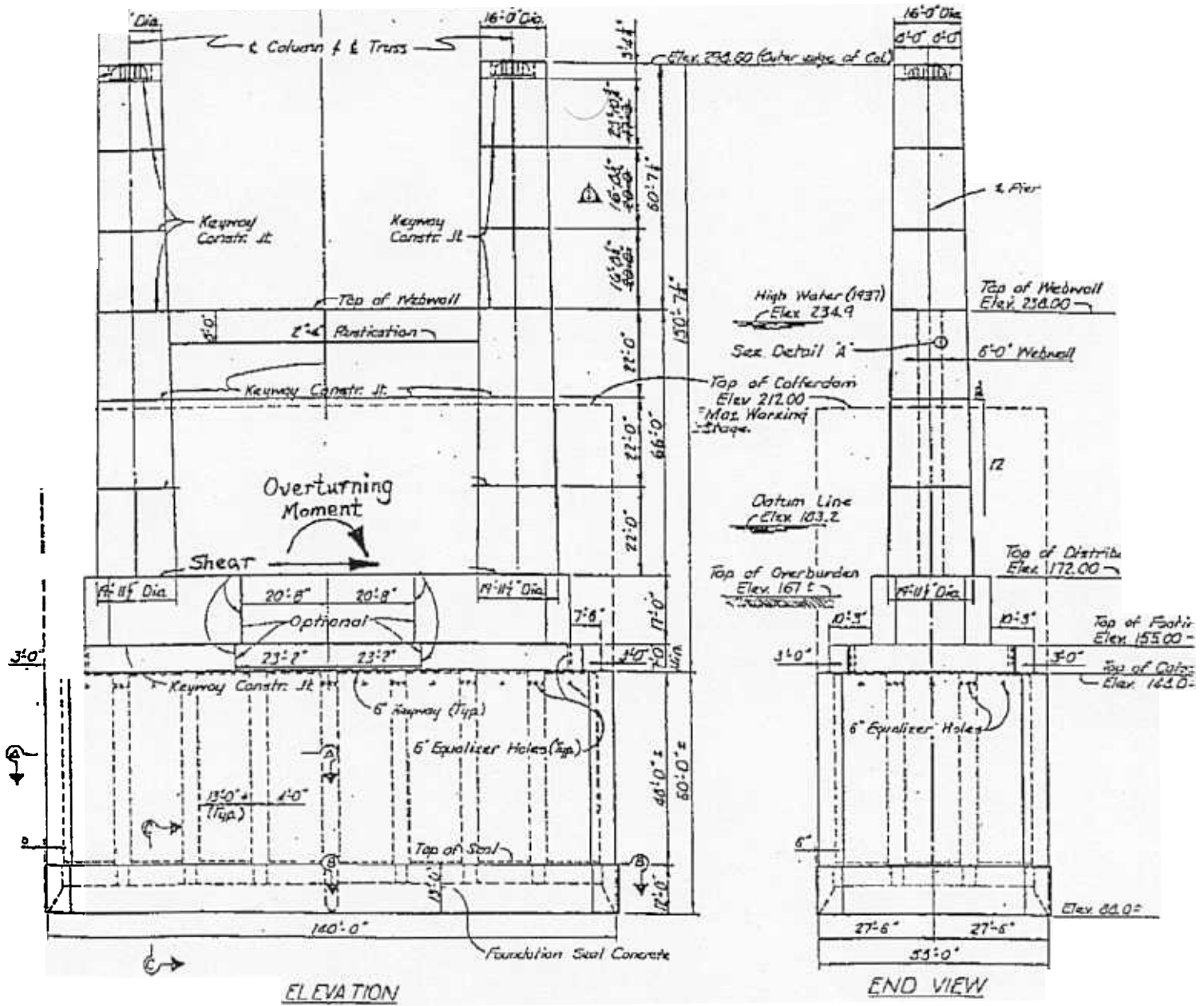
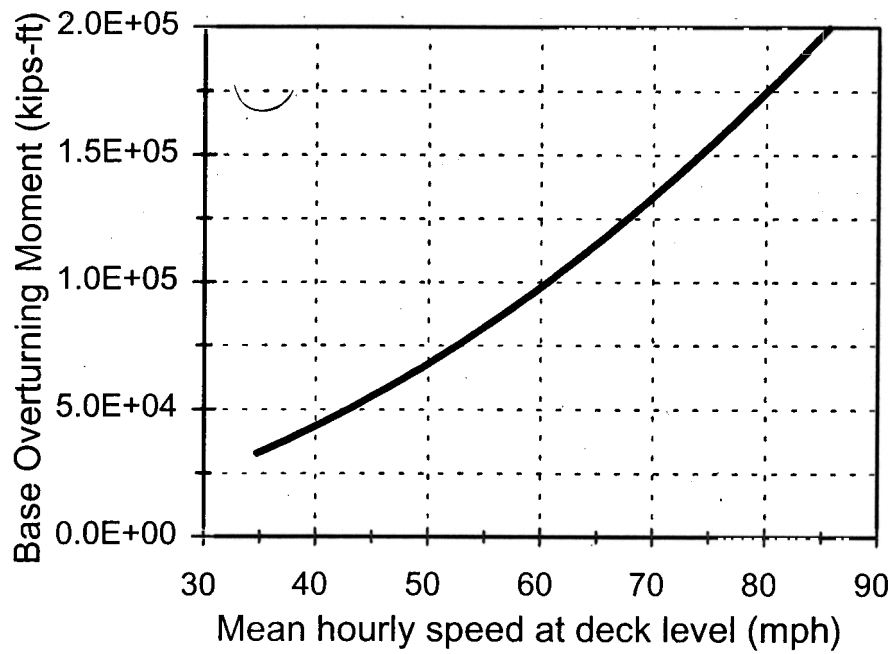
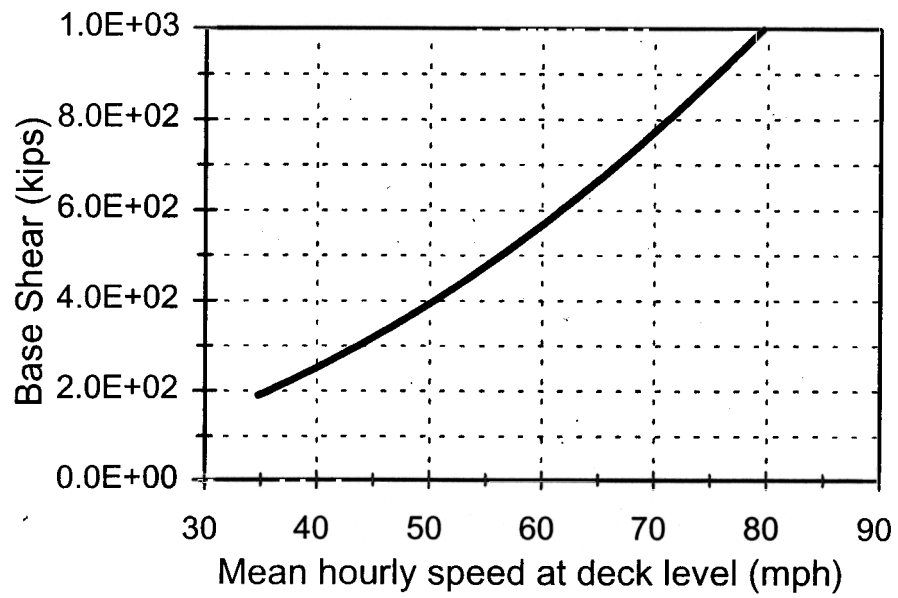
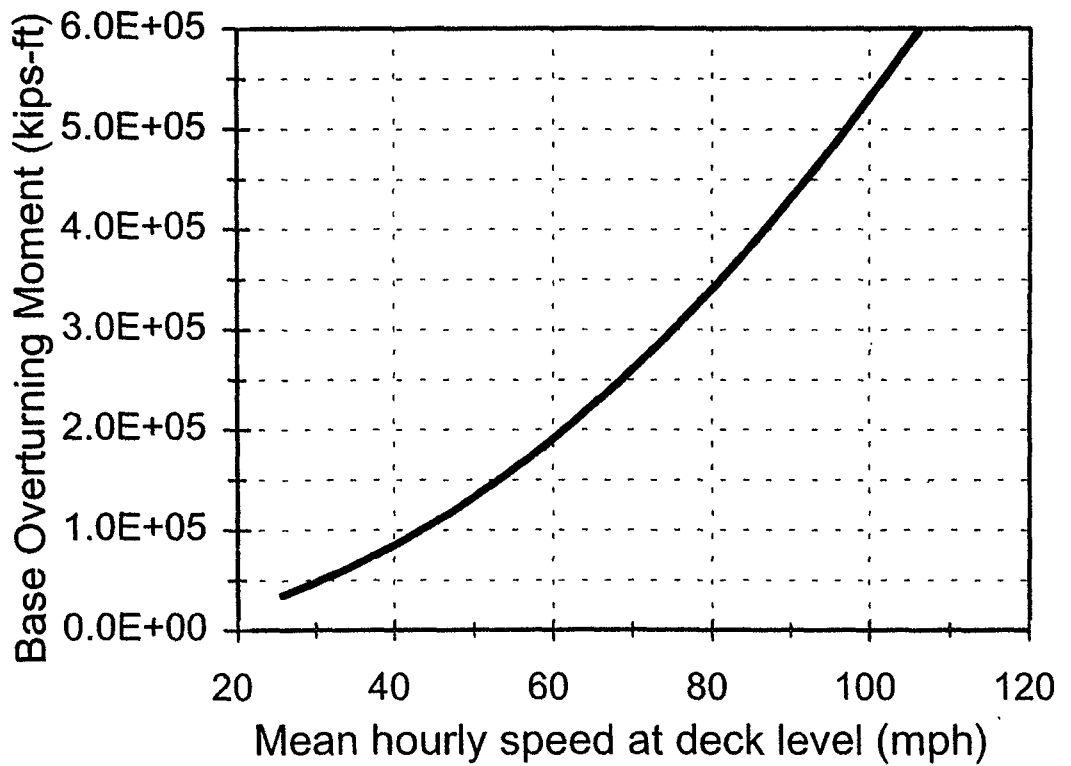
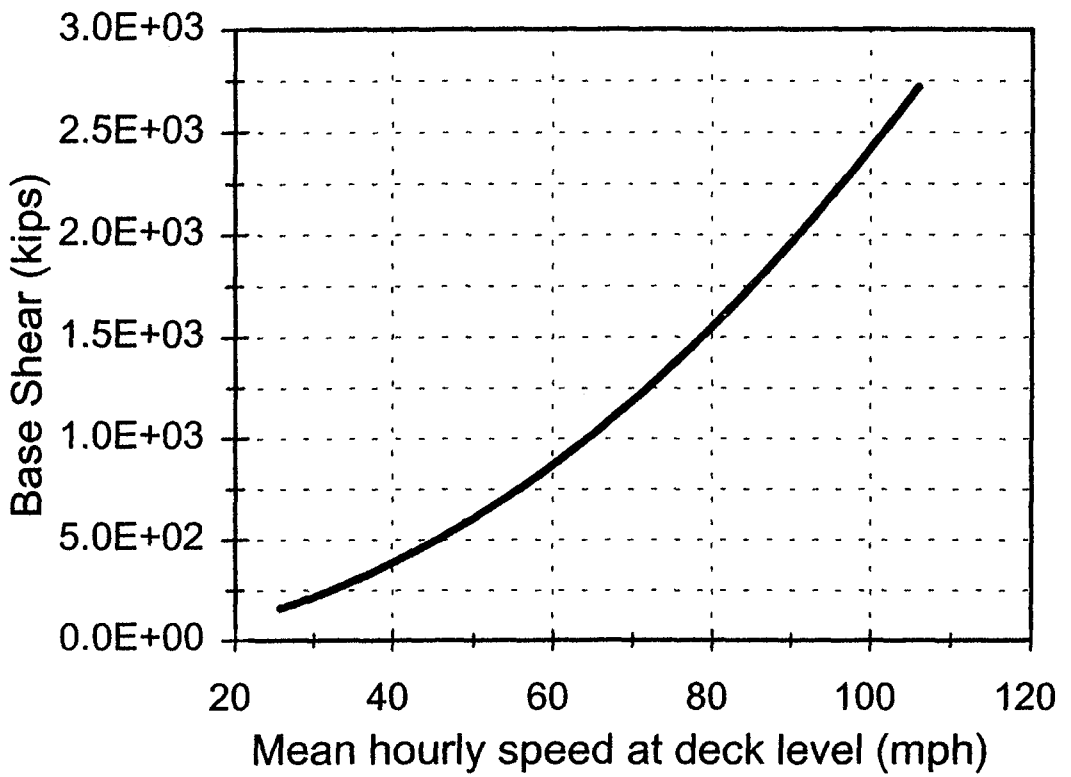


Figure 9: Definition of base loads for I-40 bridge



**Figure 10:** Base transverse loads as a function of wind speed - Maysville Bridge



**Figure 11:** Base transverse loads as a function of wind speed - I-40 Bridge

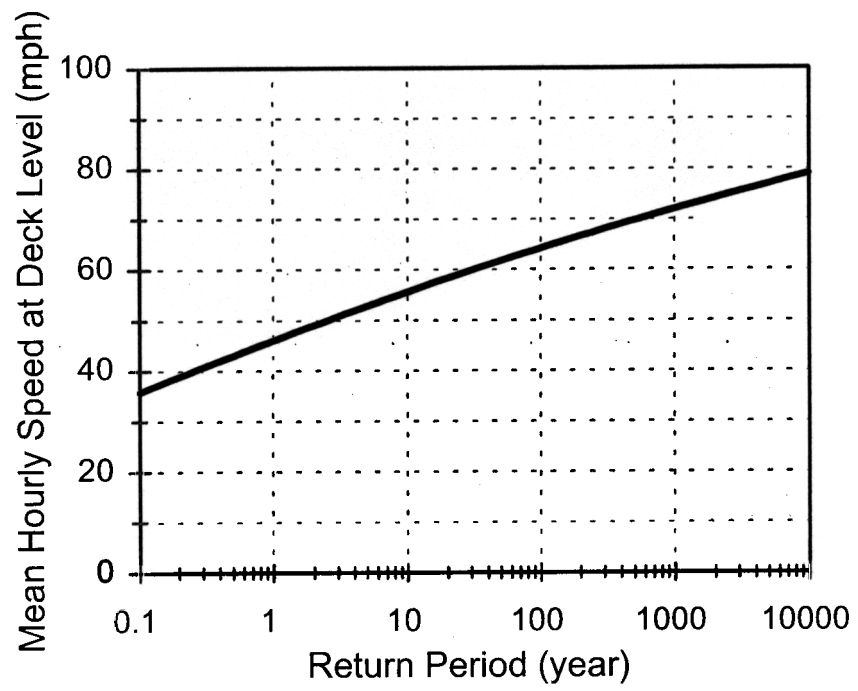


**Figure 12:** Return period wind speed for Maysville Bridge

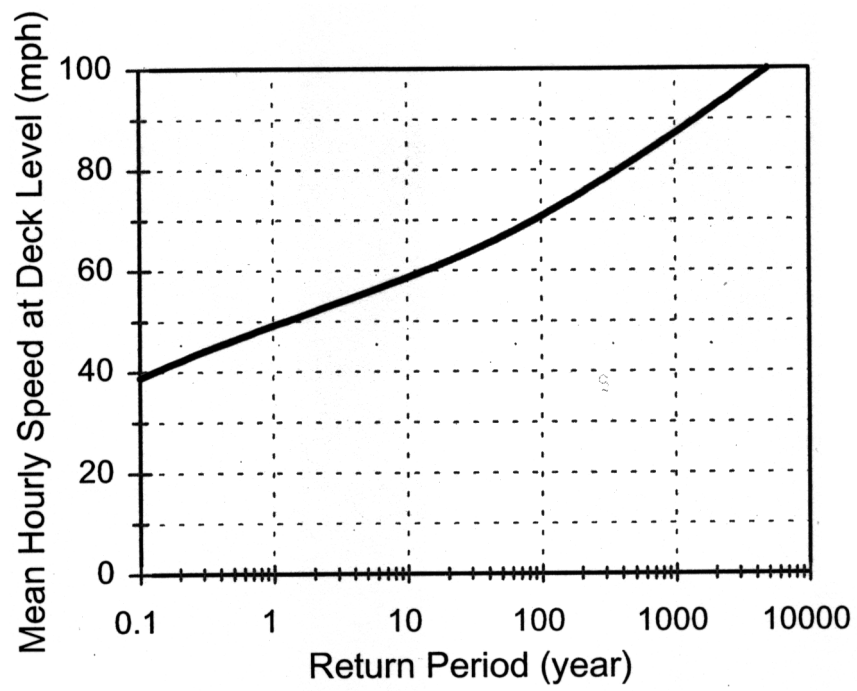
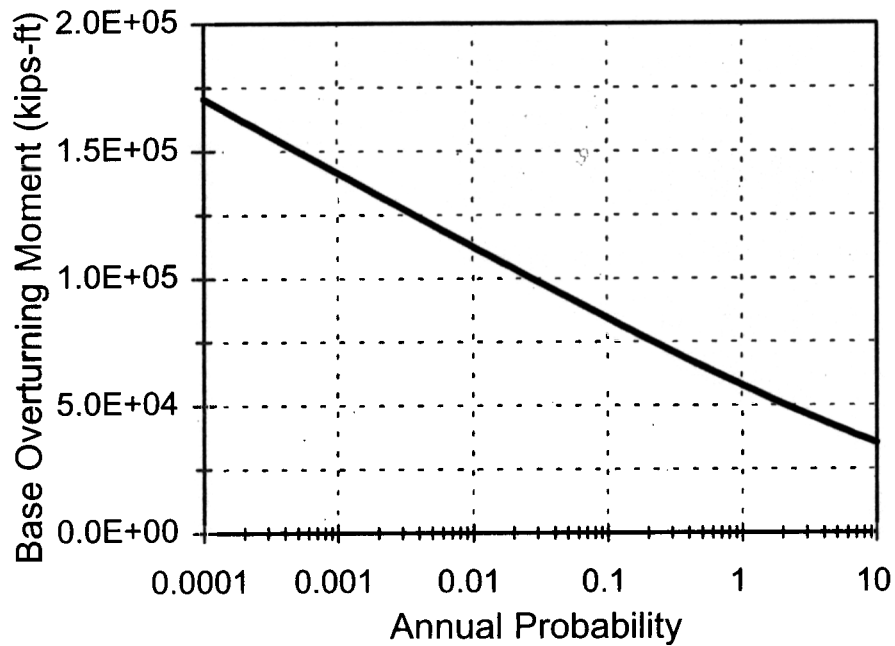
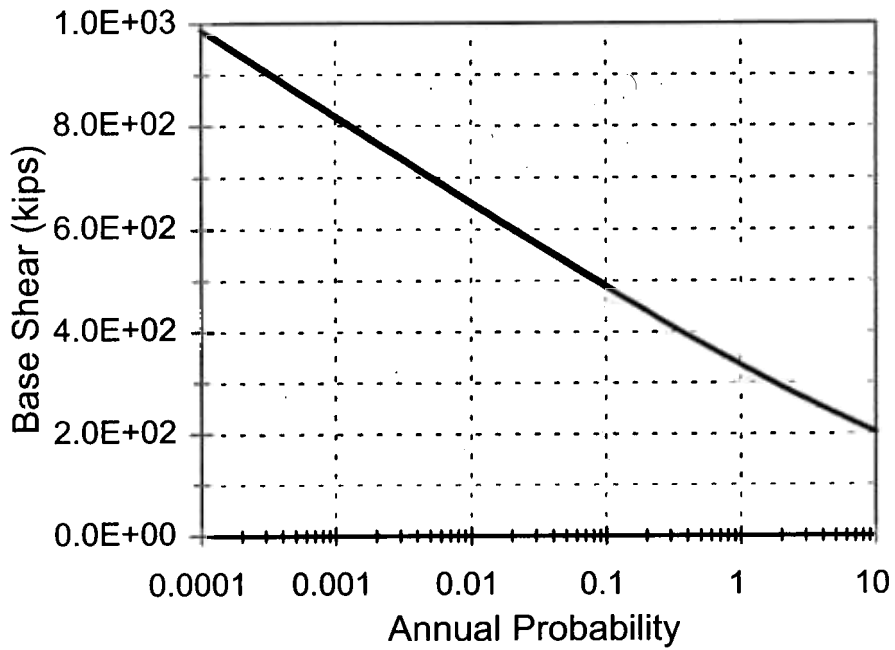
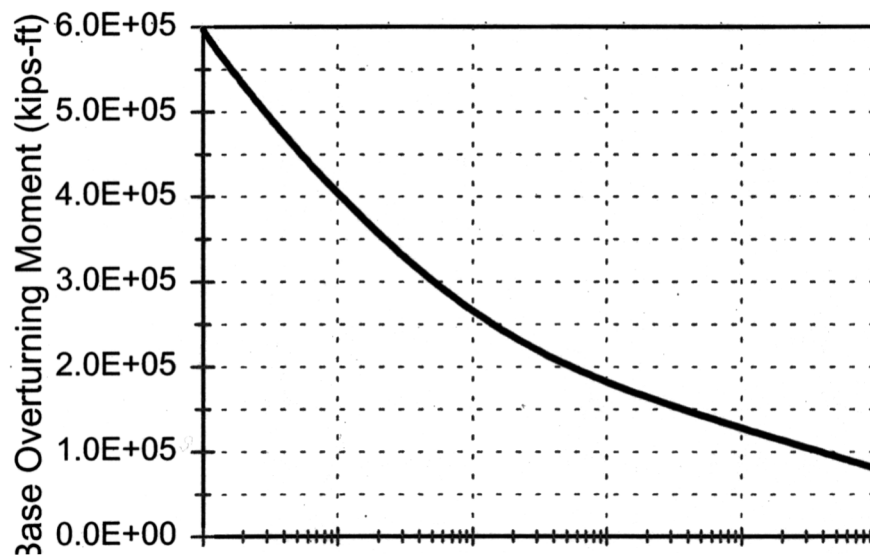
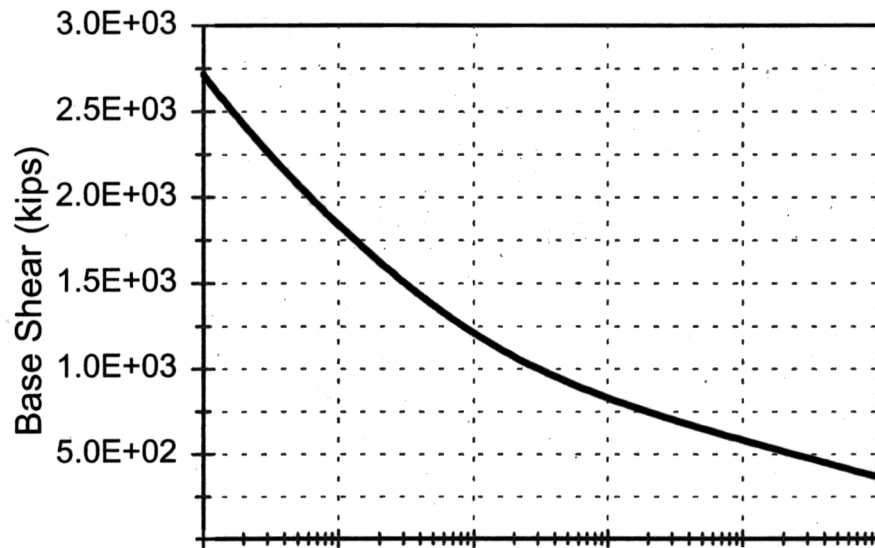


**Figure 13:** Return period wind speed for I-40 Bridge



**Note:** The annual probability is defined in the same way as ASCE 7-98. Therefore, an annual probability of 0.02 corresponds to a 50-year return period and 0.01 corresponds to a 100-year return period. Values greater than 1 indicate the number of events per year.

**Figure 14:** Base transverse loads as a function of annual probability  
- Maysville Bridge



Annual Probability

**Note:** The annual probability is defined in the same way as ASCE 7-98. Therefore, an annual probability of 0.02 corresponds to a 50-year return period and 0.01 corresponds to a 100-year return period. Values greater than 1 indicate the number of events per year.

**Figure 15:** Base transverse loads as a function of annual probability  
- I-40 Bridge